Structure of the uncomplexed *Neisseria meningitidis* factor H-binding protein fHbp (rLP2086)

Laura Cendron,[a,b]***** **Daniele Veggi,**[c] **Enrico Girardi**[a]‡ **and Giuseppe Zanotti**[a,b]

[a]Department of Biological Chemistry, University of Padua, Viale G. Colombo 3, 35121 Padua, Italy, [b]Venetian Institute of Molecular Medicine (VIMM), Via Orus 2, 35129 Padua, Italy, and [c]Novartis Vaccines and Diagnostics, 53100 Siena, Italy

‡ Present address: La Jolla Institute for Allergy and Immunology, 9420 Athena Circle, La Jolla, CA 92037, USA.

Correspondence e-mail: laura.cendron@unipd.it

fHbp, a highly immunogenic outer membrane protein of *Neisseria meningitidis*, is responsible for binding to human factor H, a multi-domain protein which is the central regulator of the alternative complement pathway. Here, the crystal structure of mature fHbp determined at 2 Å resolution is presented and is compared with the structure of the same protein in complex with factor H domains 6 and 7 recently solved using X-ray techniques. While the overall protein fold is well conserved, modifications are observed mainly in the loop regions involved in the interaction, reflecting a specific adaptation of fHbp in complexing factor H with high affinity. Such a comparison has to date been impaired by the fact that fHbp models determined by NMR show remarkable differences over the entire structure.

1. Introduction

Neisseria meningitidis factor H-binding protein (fHbp) is a promising surface-exposed antigen that is currently under intensive investigation for the development of effective meningococcal serogroup B vaccines, which are now undergoing clinical trials (Mascioni *et al.*, 2009). fHbp is a highly immunogenic universally expressed lipoprotein that is capable of enhancing serum resistance by the bacterium (Pizza *et al.*, 2008). The rational formulation of vaccines based on antigens such as fHbp, alone or in combination with other antigens, could overcome the limitations of the use of the capsular polysaccharides conjugate approach, which has proven to be problematic for group B meningococci.

fHbp, also known as GNA1870, was first identified by reverse vaccinology during screening of the MC58 *N. meningitidis* strain and was subsequently characterized by biochemical methods and designated rLP2086 (Masignani *et al.*, 2003). Subsequently, it was discovered to confer bacteria with the capability to bind the factor H multi-domain protein, which is an essential downregulatory modulator of the alternative complement pathway (Madico *et al.*, 2006). Using this mechanism, fHbp gives meningococci the opportunity to evade complement-dependent killing, which defines a critical step in the innate immune defences against bacterial infections. Moreover, the detection of fHbp in all meningococcal strains examined to date, although at different expression levels, makes it a lead candidate for a vaccine. Comparison of all the different fHbp sequences analyzed allowed the identification of three main variants of this lipoprotein which share at least 63% sequence identity, with higher sequence conservation within the three subgroups. Other authors have classified its genetic variation as divided into two subfamilies, one of which includes the two variants with higher identity (Jacobsson *et al.*, 2006; Bambini *et al.*, 2009).

The fHbp protein precursor undergoes N-terminal signal sequence processing and lipidation at the cysteine residue present within a lipobox motif (-L*xx*C-) to allow its surface exposure and lipid-mediated anchoring to the outer membrane (Fletcher *et al.*, 2004). A modular assembly characterizes its structure. Two major and apparently unrelated domains assemble to form the overall three-dimensional
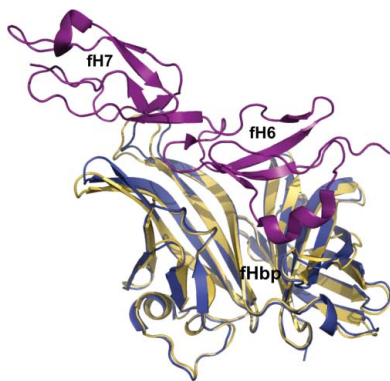
structural communications

X-ray data	
Space group	$P3_121$
Unit-cell parameters (Å)	$a = b = 83.097, c = 71.301$
Resolution (Å)	36.0–2.0 (2.2–2.0)
Independent reflections	17912 (2010)
Multiplicity	3.9 (3.6)
Completeness (%)	98.0 (90.7)
$\langle I/\sigma(I) \rangle$	6.6 (1.8)
R_{merge}	0.221 (0.474)
Refinement	
Total No. of atoms, including solvent	2017
Mean B value (Å^2)	30.6
R_{cryst} (%)	22.8
R_{free} (%)	25.0
Ramachandran plot (%)	
Most favoured	87.5
Additionally allowed	12.5
Generously allowed	0
R.m.s.d. bond lengths (Å)	0.023
R.m.s.d. bond angles (°)	1.5

architecture and both are involved in defining the factor H binding surface, as demonstrated by the recently published structure of factor H domains 6 and 7 (fH67) in complex with fHbp (Schneider *et al.*, 2009). Here, we report the crystallization and X-ray structure determination of the *N. meningitidis* factor H binding protein alone at 2.0 Å resolution, enabling us to compare it with the same protein in complex with factor H domains 6 and 7 and to map the main rearrangements that fHbp undergoes upon complex formation.

2. Materials and methods

2.1. Protein purification and crystallization

Mature recombinant fHbp from Val73 to Gln320 (numbering system according to Schneider *et al.*, 2009), *i.e.* lacking the lipid-anchoring motif, was expressed in *Escherichia coli* and purified by cation-exchange chromatography (SP HP, GE Healthcare) using 50 m*M* sodium acetate pH 5.5 as the binding buffer and 50 m*M* sodium acetate, 1 *M* NaCl pH 5.5 as the elution buffer. Subsequently, a second hydrophobic chromatography purification step (HIC, Butyl-Sepharose, GE Healthcare) allowed recovery of the protein in the flowthrough. The sample was finally dialyzed against a buffer consisting of 20 m*M* MES, 100 m*M* NaCl pH 6.5 and concentrated to 30 mg ml^{-1} for crystallization trials. A sparse-matrix approach was used at both 293 and 277 K, combining all of the most popular crystallization kits. After approximately two months of incubation, a bunch of rod-shaped crystals grew in the presence of 25% PEG 2000 MME, 300 m*M* sodium acetate, 100 m*M* Tris pH 7.5 at 293 K to a maximum size of 0.3 mm along one axis. Despite being poorly reproducible, the crystal quality and dimensions could be improved by multiple seeding attempts.

2.2. Structure determination

The best data set was collected at the Elettra synchrotron-radiation source (XRD1 beamline) in Trieste, Italy. Before data collection, the protein crystals were soaked for few seconds in a cryoprotectant solution (15% ethylene glycol, 25% PEG 2000 MME, 300 m*M* sodium acetate, 100 m*M* Tris pH 7.5) and flash-frozen in a cryogenic nitrogen stream at 100 K. The best crystals diffracted to 2 Å resolution.

fHbp crystallized in space group $P3_121$, with unit-cell parameters $a = b = 83.10, c = 71.30$ Å. The diffraction data were processed with *MOSFLM* and *SCALA*. The asymmetric unit contained a single monomer, corresponding to a Matthews coefficient of 2.7 Å^3 Da^{-1} and a solvent content of approximately 54% of the crystal volume. Analogously to the report of Schneider *et al.* (2009), molecular-replacement trials using NMR models of either the C-terminal barrel (PDB entry 1ys5; Cantini *et al.*, 2006) or the entire protein (PDB entries 2kc0 and 2kdy; Mascioni *et al.*, 2009, 2010) of fHbp failed. The
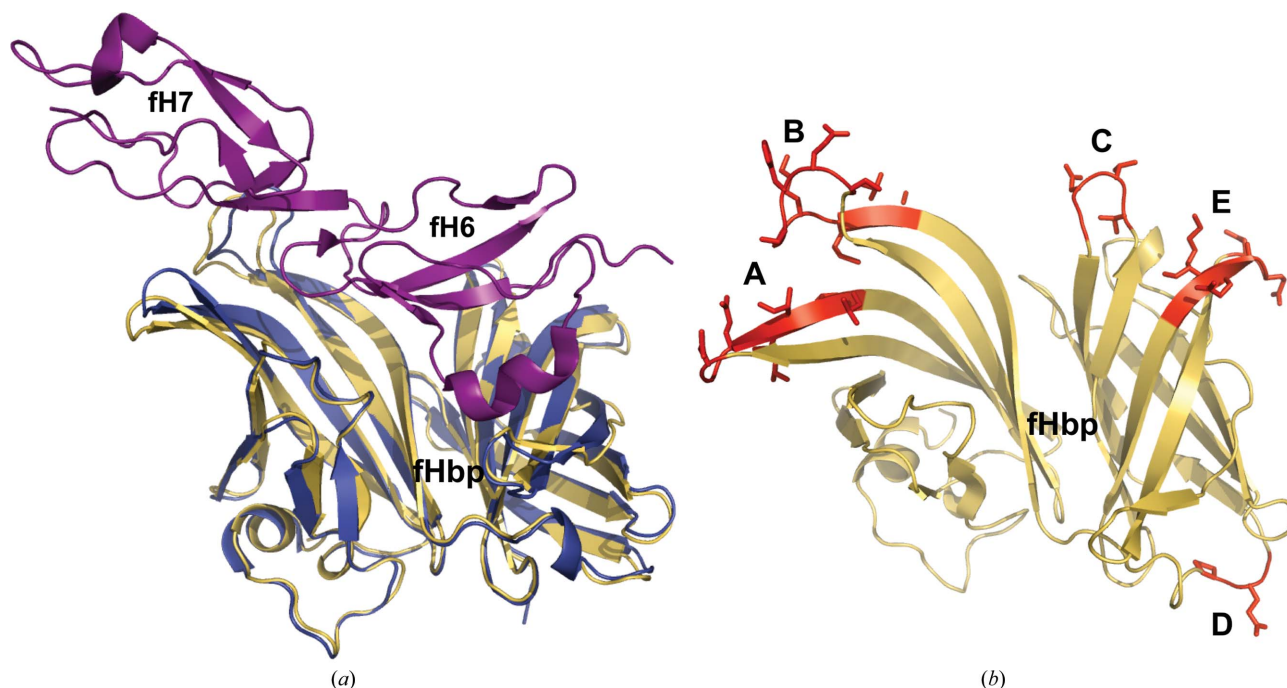

Figure 1
Superposition of the cartoon models of the fHbp monomer alone (yellow) and in complex (light blue). The model of factor H domains 6 and 7 (magenta) is positioned in the upper part of the picture in (*a*), while it is omitted in (*b*). The fragments that undergo major displacements are highlighted in red in (*b*).

correct solution was finally found by the *Phaser* software (McCoy *et al.*, 2007) using a model of fHbp in complex with the two domains fh6 and fh7 (CCP6 and CCP7) of the complement control protein factor H (PDB entry 2w80; Schneider *et al.*, 2009) determined by X-ray diffraction. Several cycles of automatic refinement in *REFMAC* (Murshudov *et al.*, 1997) and manual model building in *Coot* (Emsley & Cowtan, 2010) reduced the crystallographic R factor to a final value of 0.228 (R_{free} of 0.250) for all data from 36 to 2.0 Å resolution. Defined electron density was present for residues Ala79–Gln320, whilst the first seven residues of the recombinant construct are possibly flexible and could not be fitted in the electron density. Data-processing and refinement statistics are presented in Table 1.

3. Results and discussion

The overall fold of the fHbp model fits well to the structure of the same protein in complex with complement factor H domains fH6 and fH7 (PDB entries 2w80 and 2w81; Schneider *et al.*, 2009), thus supporting the idea that in both cases the structure is not forced or distorted by the crystal packing. fHbp consists of two β-barrel domains with different topologies, spanning the fragments 79–202 (formerly domain A and the initial part of domain B) and 202–320

Figure 2
(a) Superposition of C^{α} atoms of the unliganded fHbp structure (PDB entry 3kvd; this paper) and the following models: fHbp model 1 (2kc0; NMR; red), fHbp in complex with fH domains 6 and 7 (PDB entry 2w80; blue), the seven independent copies present in the asymmetric unit of fHbp in complex with fH domains (PDB entry 2w81; other colours). (b) Distances calculated by C^{α}-atom superposition of the fHbp model alone (PDB entry 3kvd; this paper) with all the models included in the 2kc0 NMR ensemble.

(the remainder of domain B and domain C), connected by a short loop (numbering system according to Schneider *et al.*, 2009) (Fig. 1).

The two barrels associate together mainly by hydrophobic inter-actions. The exposed surface buried upon association is about 3560 Å^2, which represents about 30% of the total surface of the two domains. The remaining protein surface (about 8315 Å^2) is char-acterized by a prevalence of clusters of positively and negatively charged residues exposed to the solvent, which confer a strongly hydrophilic nature on the protein.

A comparison of the structures of the fHbp protein alone (PDB entry 3kvd) and in complex with fh6 and fh7 domains (PDB entry 2w80) indicates that three loops undergo significant shifts upon complex formation, reaching maximum root-mean-square deviations (r.m.s.d.s) between equivalent C^{α} atoms greater than 2 Å: fragment *A*, which connects β-sheets 5 and 6a (residues 149–155), fragment *B*, which is located in a loop within β-sheets 7 and 8a (residues 182–188), and fragment *C*, which corresponds to the loop that links β-sheets 15b and 16 (residues 307–310) (Figs. 1 and 2).

Other less pronounced shifts (maximum r.m.s.d. greater than 1.2 Å) are observed in the regions between Pro210 and Gly212, just before the linker between the two fHbp β-barrels (fragment *D*), between Asn280 and Gly285, which is part of β-sheet 14 (fragment *E*), and locally for residue Leu96. Except for fragment *D* and Leu96, all of these fragments are part of the fHbp surface that is involved in extensive interactions with factor H domains 6 and 7 in the com-plexed fHbp (PDB entry 2w80).

While fragments *A* and *B* are implicated in interactions with factor H domain 7, fragment *C* is located right after residues Glu304 and Lys306 (β-sheet 15b) which interact with factor H domain 6.

In particular, a large network of hydrogen bonds is established between factor H domain 7 and fHbp residues spanning the loop from Gln180 to Arg195, the core of which (Ser182–Met188, fragment *B*) also encounters large shifts in the unliganded form described here. Analogously, fragment *E*, which is part of β-sheet 14 of the fHbp protein, is slightly shifted upon fh6-domain binding, allowing the formation of multiple hydrogen bonds and salt bridges between the two interaction partners as the result of a general adaptation of the whole region including β-sheets 13 and 14 and the connecting loop. Fragments *A* and *C*, in contrast, despite being part of the contact surface, are involved in rather loose interactions in the liganded form (fHbp–fh6/7 complex).

Interestingly, in the structure of uncomplexed fHbp, fragments *A* and *C* are involved in crystal-packing contacts with the same loops of symmetry-related molecules, while fragment *B* is exposed to solvent. While the protein–protein contacts between fHbp molecules in the crystals point towards a reduced relevance of the observed rearrangements concerning fragments *A* and *C*, they certainly allow the inference of a degree of plasticity and a propensity to interact with other protein surfaces. In contrast, the lack of crystal contacts involving fragment *B* strongly suggests that the rearrangement of this loop observed in the liganded form can be ascribed to fHbp–fh6/7 binding.

Finally, a few weak adjustments regarding the overall fHbp struc-ture (Fig. 1*b*) could represent a general adaptation/contraction of this bacterial recognition factor on interaction with factor H.

To further evaluate the relevance of the observed rearrangements, all of the models of the independent copies of the complexed fHbp present in the asymmetric unit of the two crystal forms (PDB entries 2w80 and 2w81) were also compared, taking one of them as the reference structure. As can be seen in Fig. 2(*a*), rearrangements between the isolated fHbp and one of the forms in the complex are much larger than the weak shifts observed within the independent
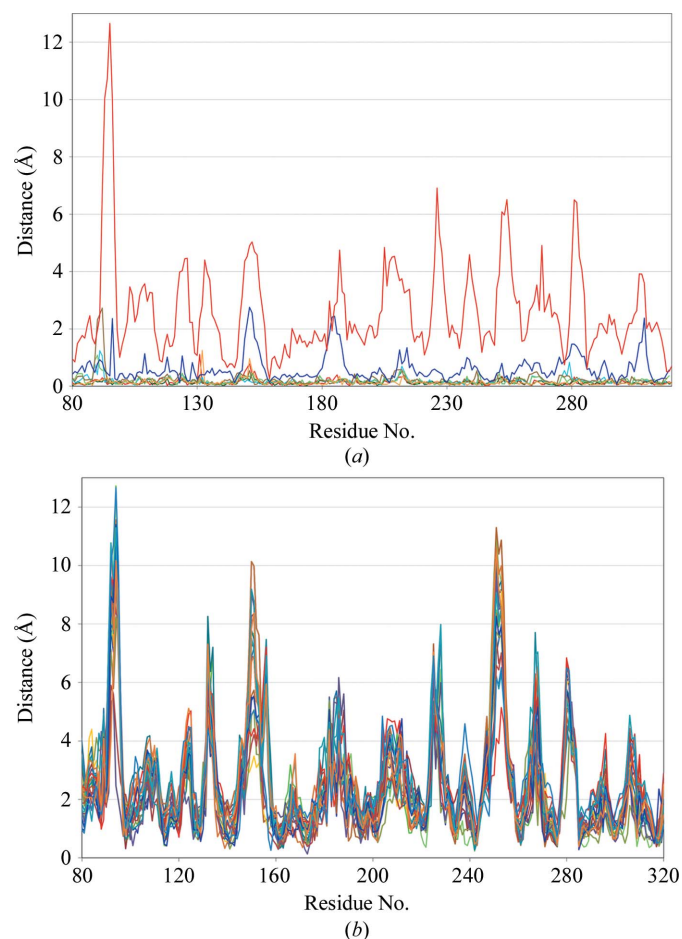
models of complexed fHbp, where the calculated r.m.s.d. never exceeds 0.5–0.8 Å. A limited set of residues from Asp90 to Asp93 represent the only exception and are grouped in a flexible region far from the interaction surface involved in the complex. This comparison confirms that the two fHbp domains maintain the same relative organization and orientation and the only shifts that reflect meaningful and specific adaptation of fHbp to factor H domains pertain to specific loops which define the contact surface and are responsible for its very high affinity.

The NMR family of models (Cantini et al., 2006) and the X-ray structure described in this paper share the same overall fold: equivalent Cᵅ atoms of NMR model 1 superimpose with those of the crystal structure with an average r.m.s.d. of 2.6 Å. Comparable values were obtained with all of the other 24 NMR models in the 2kc0 ensemble of structures, with the highest r.m.s.d. corresponding to 2.84 Å and the lowest to 2.15 Å. However, a more careful comparison of the fHbp structures obtained using the two different techniques shows significant deviations to be present throughout the sequence, with r.m.s.d. peaks reaching values higher than 10 Å, as shown in Figs. 2(b) and 3. The divergences between the models do not only involve the connection loops; important shifts are also experienced by some of the β-strands defining the core of each of the two domains and also the small α-helical contribution present in the C-terminal domain. Similar results were obtained from the superimposition of the crystal structure of fHbp and all of the NMR models belonging to the same family (PDB entry 2kc0; Fig. 2b). These results justify a posteriori the failure in the use of the NMR models as a template for molecular replacement. It is not possible to exclude that the discrepancies between the NMR and the X-ray structure of the isolated fHbp molecule are a consequence of different experimental conditions (solvent, concentration, pH etc.) or that they reflect multiple states of the protein in solution. However, analogous important rearrangements have never been observed in any of the structures of fHbp in complex with factor H domains 6 and 7, where the experimental conditions are independent of those described in this paper and the observed structural changes, if compared with the fHbp X-ray structure, are clear but strictly confined to the loops embracing the interaction partner.

A wide-ranging structural comparison of both the entire structure of fHbp and the two subdomains separately has been also performed against the full database of structures deposited in the PDB using the ProFunc (Laskowski et al., 2005) and DALI (Holm & Park, 2000) servers. The N-terminal subdomain shows only weak similarity to the protein streptavidin, while interesting similarities are found between the C-terminal fHbp subdomain and the membrane-domain structure of an engineered triple mutant of the OmpA protein from E. coli (OmpA171t; PDB entry 1qjp; Pautsch & Schulz, 1998). More generally, the C-terminal fHbp domain shares the folding of classical porins, such as the NspA antigen from N. meningitidis itself (Lewis et al., 2010). A superposition of our model with OmpA indicates that the C-terminal fHbp subdomain (residues 202–320) fits well with the the eight-stranded antiparallel β-barrel of OmpA, while it differs in terms of the extension and orientation of the more flexible loops connecting the all-next-neighbour β-sheets. In particular, the shortest turns on one side of OmpA point towards the periplasmic space, whilst the longer flexible turns are at the external end. Although there is a structural similarity between the fHbp carboxy-terminal barrel and the OmpA protein, the localization of the two proteins is radically different, with fHbp being completely exposed on the cell surface of the meningococcus and only anchored to the outer membrane through the lipidated moiety (Mascioni et al., 2010). Interestingly, some porins are ligands for human factor H on gonococci, while meningococci have adapted the multi-domain and lipid-anchored fHbp to bind to factor H and enhance the bacterial ability to evade complement-dependent killing (Welsch & Ram, 2008).

4. Conclusions

The crystal structure of mature recombinant fHbp (79–202) described here completes the set of structural data available on this fascinating vaccine candidate and has important implications for the development of novel therapeutic agents against N. meningitidis. Our model allowed us not only to map the main rearrangements that the protein undergoes upon human factor H binding, but also to analyze the significant discrepancies that are observed between the currently available NMR models and X-ray structures. As it has been widely discussed, the fHbp lipoprotein does not undergo dramatic structural changes upon interaction with factor H. However, the major shifts deduced from superimposition of the apo form (this paper) and the complexed form (PDB entries 2w80 and 2w81) pertain mainly to three loops that are localized near the complex interface, suggesting a significant, although limited, plasticity of this protein during factor H binding. Moreover, given the extremely promising vaccine potential already demonstrated by fHbp, the unliganded fHbp structure described here is fundamental to the characterization of the antigenic epitopes exposed on its protein surface, making it a reference point for any further structural studies involving neutralizing antibodies or the development of a modified version of the protein that is able to induce efficient protective immunity.
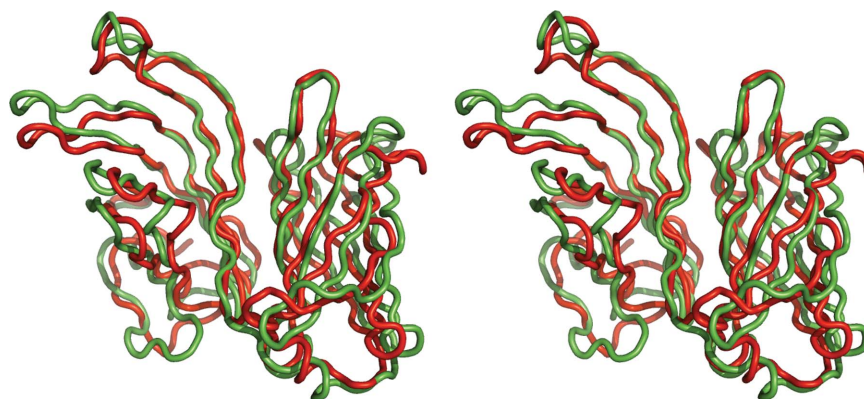

Figure 3
Cartoon tube stereoview of a superimposition of the fHbp crystal structure (PDB entry 3kvd; red) and fHbp model 1 determined by NMR (PDB entry 2kc0; green).

References

Bambini, S., Muzzi, A., Olcen, P., Rappuoli, R., Pizza, M. & Comanducci, M. (2009). *Vaccine*, **27**, 2794–2803.

Cantini, F., Savino, S., Scarselli, M., Masignani, V., Pizza, M., Romagnoli, G., Swennen, E., Veggi, D., Banci, L. & Rappuoli, R. (2006). *J. Biol. Chem.* **281**, 7220–7227.

Emsley, P., Lohkamp, B., Scott, W. G. & Cowtan, K. (2010). *Acta Cryst.* D**66**, 486–501.

Fletcher, L. D., Bernfield, L., Barniak, V., Farley, J. E., Howell, A., Knauf, M., Ooi, P., Smith, R. P., Weise, P., Wetherell, M., Xie, X., Zagursky, R., Zhang, Y. & Zlotnick, G. W. (2004). *Infect. Immun.* **72**, 2088–2100.

Holm, L. & Park, J. (2000). *Bioinformatics*, **16**, 566–567.

Jacobsson, S., Thulin, S., Mölling, P., Unemo, M., Comanducci, M., Rappuoli, R. & Olcén, P. (2006). *Vaccine*, **24**, 2161–2168.

Laskowski, R. A., Watson, J. D. & Thornton, J. M. (2005). *Nucleic Acids Res.* **33**, W89–W93.

Lewis, L. A., Ngampasutadol, J., Wallace, R., Reid, J. E., Vogel, U. & Ram, S. (2010). *PLoS Pathog.* **6**, e1001027.

Madico, G., Welsch, J. A., Lewis, L. A., McNaughton, A., Perlman, D. H., Costello, C. E., Ngampasutadol, J., Vogel, U., Granoff, D. M. & Ram, S. (2006). *J. Immunol.* **177**, 501–510.

Mascioni, A. *et al.* (2009). *J. Biol. Chem.* **284**, 8738–8746.

Mascioni, A. *et al.* (2010). *Biochim. Biophys. Acta*, **1798**, 87–93.

Masignani, V. *et al.* (2003). *J. Exp. Med.* **197**, 789–799.

McCoy, A. J., Grosse-Kunstleve, R. W., Adams, P. D., Winn, M. D., Storoni, L. C. & Read, R. J. (2007). *J. Appl. Cryst.* **40**, 658–674.

Murshudov, G. N., Vagin, A. A. & Dodson, E. J. (1997). *Acta Cryst.* D**53**, 240–255.

Pautsch, A. & Schulz, G. E. (1998). *Nature Struct. Biol.* **5**, 1013–1017.

Pizza, M., Donnelly, J. & Rappuoli, R. (2008). *Vaccine*, **26**, I46–I48.

Schneider, M. C., Prosser, B. E., Caesar, J. J., Kugelberg, E., Li, S., Zhang, Q., Quoraishi, S., Lovett, J. E., Deane, J. E., Sim, R. B., Roversi, P., Johnson, S., Tang, C. M. & Lea, S. M. (2009). *Nature (London)*, **458**, 890–893.

Welsch, J. A. & Ram, S. (2008). *Vaccine*, **26**, I40–I45.